CYCLIC PERFORMANCE AND RETROFIT DESIGN OF PRE-NORTHRIDGE STEEL MOMENT CONNECTION WITH WELDED HAUNCH

Qi-Song YU[1] And Chia-Ming UANG[2]

SUMMARY

The effectiveness of using welded haunch scheme to rehabilitate pre-Northridge steel moment connections was investigated through cyclic testing of two full-scale specimens−one of them incorporated a lightweight concrete slab. Experimental results demonstrated that with the low-toughness E70T-4 groove weld in place, welding a triangular haunch beneath the beam's bottom flange significantly improved the seismic performance of steel moment connections. When a concrete slab was present, brittle fracture of the welded joints was prevented. A simplified model which considered the force equilibrium and deformation compatibility between the steel beam and the haunch was developed to predict the stress level in the beam flange groove welds. A design procedure for the welded haunch connection was proposed.

INTRODUCTION

Steel special moment-resisting frames (SMRFs), believed to be capable of dependable and ductile response during strong earthquakes, have long been considered a premier lateral force-resisting system. Unfortunately, widespread brittle fractures in or around the beam bottom flange to column flange groove weld were observed in more than 150 steel SMRF buildings after the January 17, 1994 Northridge earthquake. Among the concerns regarding the poor performance of these connections is the ability to economically rehabilitate steel moment connections in existing buildings.

RESEARCH OBJECTIVES AND SCOPE

The objective of this research was to investigate the effectiveness of using welded haunch for connection modifications. Two full-scale specimens were tested. One specimen (designated as NIST-2) was bare steel and the other one (designated as NIST-2C) incorporated a lightweight concrete slab. Based on the research findings, design procedure for the welded haunch modification was also developed [Yu et al. 1997].

TEST SPECIMENS AND TESTING PROCEDURE

The specimen geometry and test setup are shown in **Figure 1**. Two nominally identical pre-Northridge steel beam-to-column subassemblies were first constructed for modification. See **Table** 1 for actual material properties. The moment connections (see **Figure 2**) were designed in accordance with the 1985 Uniform Building Code [*Uniform* 1985]. Each specimen was constructed and inspected using techniques similar to those used in pre-Northridge construction. Beam flange groove welding was performed with a 0.12-in. diameter E70T-4 electrode (Lincoln 3M); steel backing and weld tabs were left in place. One-in. diameter A325 slip-critical high-strength bolts were fully tightened using the turn-of-nut method.

The geometry and welding details of the welded haunch for modifications are shown in **Figure** 3. A 0.072-in. diameter E71T-8 electrode (Lincoln NR-232) with a specified Charpy V-Notch toughness of 20 ft-lb at -20° F was used for making all the welds for connection modifications. The groove welded joint of the beam top flange was left in its pre-Northridge condition. A 6-1/4-in. thick, 8-ft wide lightweight concrete slab was incorporated in the composite specimen in order to simulate a common practice of composite floor slab construction in

[1] *Degenkolb Engineers, 225 Bush St.,, Suite 1000, San Francisco, CA 94104, USA Email: kyu@degenkolb.com*
[2] *University of California at San Diego, La Jolla, CA 92093-0085, USA Email: cmu@ucsd.edu*

California. Details of the concrete slab construction are shown in **Figure 4**. Nelson headed shear studs of 5-1/2-in. long, 3/4-in. in diameter, were fillet welded 12 in. on center to the beam top flange along the beam centerline. The slab consisted of a 3-1/4-in. thick lightweight concrete (f_c' = 5 ksi) on the top of the steel deck. The slab reinforcement consisted of a welded wire fabric (6×6-W1.4×W1.4) and No. 3 steel reinforcements (Grade 60).

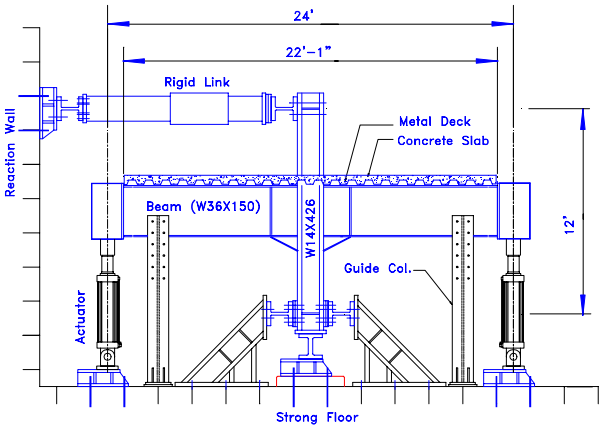

Figure 1: Test Setup

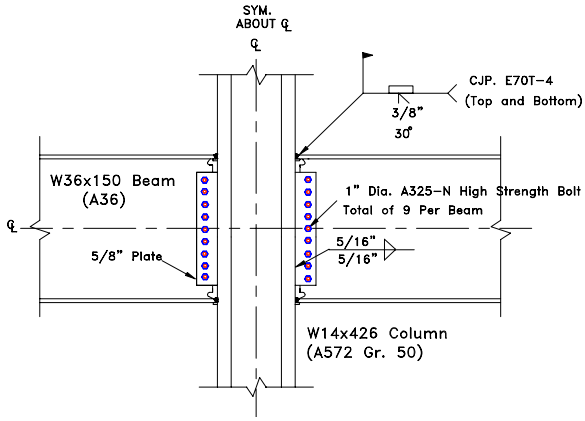

Figure 2: Pre-Northridge Connection Details

Table 1: Summary of Steel Material Characteristics

Member	Steel Type	Coupon	Fy (ksi)	Fu (ksi)
Beam W36X150	A36	Flange	49.0	69.0
		Web	47.5	65.5
Column, W14X426	A572 Gr. 50	Web	61.0	78.3
Triangular Haunch W21X93	A572 Grade 50	Flange	59.1	73.0
		Web	54.8	71.6

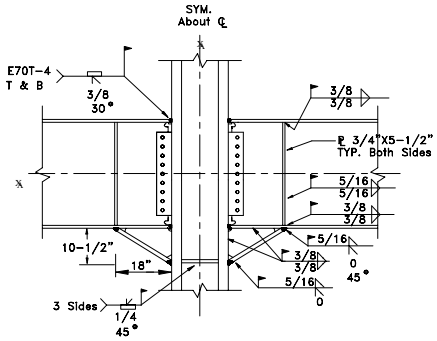

Figure 3: Details for Welded Haunch Specimens

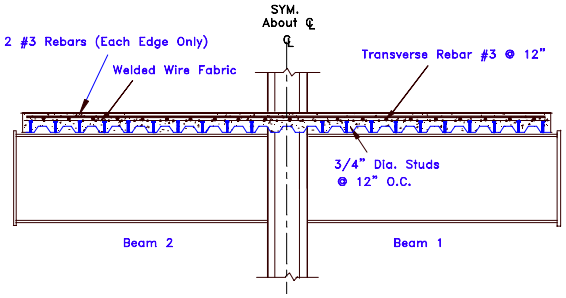

Figure 4: Composite Slab and Steel Deck Details

The ATC-24 [*Guideline* 1992] testing protocol was used for the tests. For testing purpose, a controlling value of δ_y equal to 1.2 in. was used for the test specimens. The testing was conducted in a displacement-controlled mode, i.e., equal and opposite displacements were applied to the cantilever end of the beams.

TEST RESULTS

Yielding in the bottom flanges occurred outside the haunch region. A much longer yielding length extending from the column face was observed in the top flanges [see **Figure 9**(d)]. The tendency for lateral-torsional buckling in the top flange was prevented for the composite specimen. **Figure 5**(a) shows the yielding and buckling pattern of the bare steel specimen during the $3\delta_y$ [story drift ratio (SDR) = 2.5%] cycles. The top flange groove weld of one beam fractured in the first cycle of $3\delta_y$ (SDR = 2.5%). The top flange of the other beam also experienced a similar weld fracture in the following cycle. The presence of the composite slab significantly improved the cyclic performance of the top flange welded joints. Both beams were able to complete the $4\delta_y$

(SDR = 3.3%) cycles without fracturing. **Figure 5**(b) shows the deformation configuration of the composite specimen.

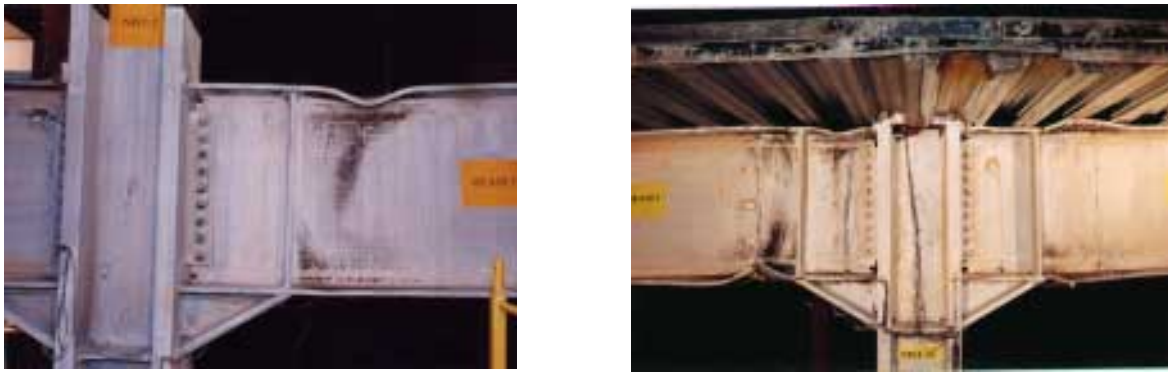

(a) Deformed Configuration of NIST-2 (b) Deformed Configuration of NIST-2C

Figure 5: Deformed Configuration of Steel Welded Haunch Specimens

Figure 6 shows the load versus beam tip displacement relationships for both specimens. The analytically predicted load versus beam tip deflection relationship obtained from ABAQUS non-linear analyses [Yu et al. 1997] correlates well with the response envelope of the test results.

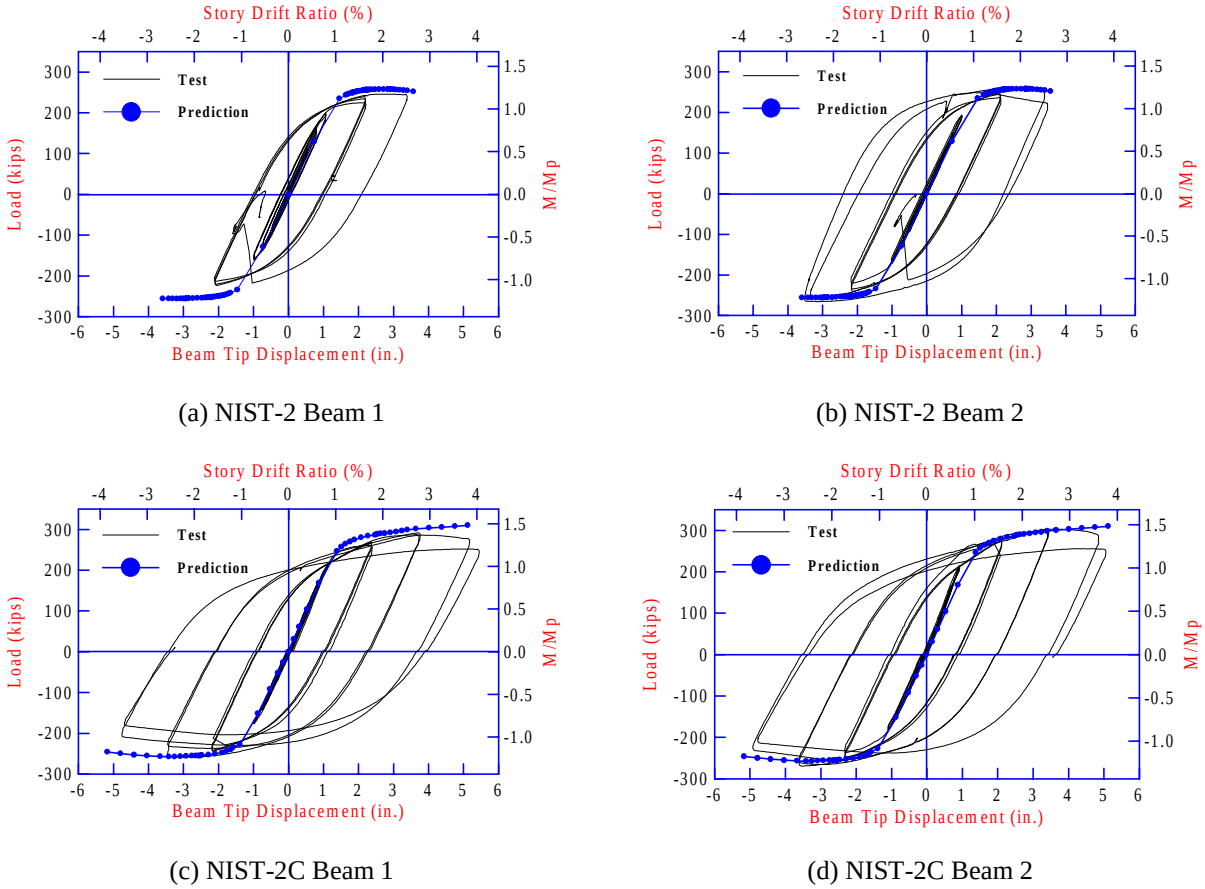

(a) NIST-2 Beam 1 (b) NIST-2 Beam 2

(c) NIST-2C Beam 1 (d) NIST-2C Beam 2

Figure 6: Load versus Beam Tip Deflection Relationships of Welded Haunch Specimens

Figure 7 summarizes the plastic rotation capacities. In addition to two large-size welded haunch specimens, another four medium-size specimens consisting of W30×99 beams, W12×279 column, and a W21×93 haunch were tested at the University of Texas, Austin [Civjan and Engelhardt 1998]. Of the three bare steel specimens (2 beams per specimen) tested, five beams experienced brittle fracture of groove weld in the top flange. Half of

the beams, however, were able to develop a plastic rotation of at least 0.018 radian. When the concrete slab was present, none of the six beams experienced weld fracture and the plastic rotation exceeded 0.025 radian, which is adequate for rehabilitation purposes [*Interim* 1995].

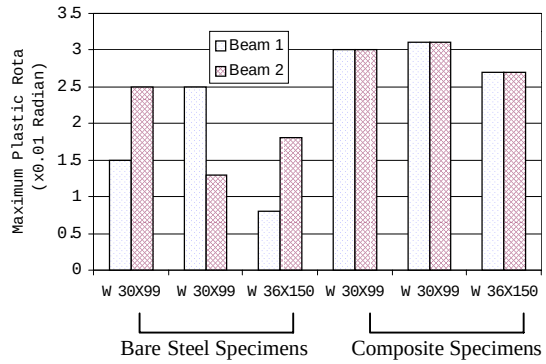

Figure 7: Comparison of Plastic Rotation Capacities

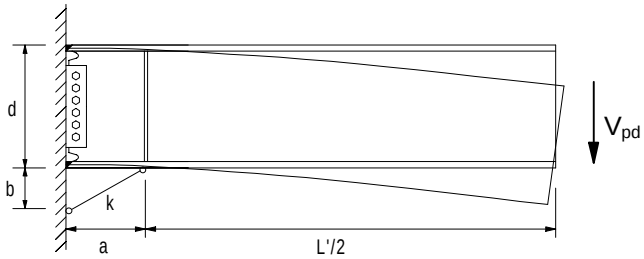

Figure 8: Simplified Mathematic Model

Simplified Model of WELDED haunch connection

Beam Moment Diagram

Figure 8 shows the simplified model of the welded haunch connection, where the haunch flange is idealized as a spring. Let the vertical component of the haunch flange axial force be βV_{pd}, where V_{pd} is the beam shear at the inflection point of the beam and β remains to be established [see **Figure 9**(a)]. The horizontal component of the haunch flange force is then equal to $\beta V_{pd}/\tan\theta$. Such a horizontal force component together with an eccentricity of $d/2$ (due to the finite depth of the beam) produces a tensile force and a concentrated moment to the beam in the haunch region [see **Figure 9**(b)]. **Figure 9**(c) shows the moment diagram of the beam alone. The moment at the haunch tip is reduced by the concentrated moment, $(\beta V_{pd}/\tan\theta)(d/2)$. When β is larger than one, the beam shear in the haunch region is reversed in direction as compared to that outside the haunch region. The reverse shear would further reduce the beam moment and, hence, the tensile stress in the top groove weld at the column face [see **Figure 9**(c)].

Deformation Compatibility between Beam and Haunch

Define x in **Figure 9**(a) as the distance of the beam section measuring from the haunch tip toward the column face. The beam bending moment in the haunch region [see **Figure 9**(c)] is:

$$M(x) = \left(\frac{L'}{2} + x\right)V_{pd} - x(\beta V_{pd}) - \left(\frac{\beta V_{pd}}{\tan\theta}\right)\frac{d}{2} \tag{1}$$

Both the bending moment and the axial force $(\beta V_{pd}/\tan\theta)$ produce a compressive stress in the beam bottom flange:

$$\sigma(x) = \frac{(L'/2 + x)V_{pd}}{I_b}\left(\frac{d}{2}\right) - \frac{x(\beta V_{pd})}{I_b}\left(\frac{d}{2}\right) - \frac{(\beta V_{pd}/\tan\theta)}{I_b}\left(\frac{d}{2}\right)^2 - \frac{\beta V_{pd}/\tan\theta}{A_b} \tag{2}$$

The horizontal component (u_B) of the beam deformation at the haunch tip is equal to the axial shortening of the beam bottom flange in the haunch region:

$$u_B = \left(\frac{L'/2 - (\beta/\tan\theta)}{EI_b}\left(\frac{d}{2}\right)^2 a + \frac{(1-\beta)a^2}{2EI_b}\left(\frac{d}{2}\right) - \frac{\beta a/\tan\theta}{EA_b}\right)V_{pd} \tag{3}$$

Using the moment-area method, where the moment is expressed in (1), the vertical component is:

$$v_B = \left(\frac{L'/2 - (\beta/\tan\theta)}{EI_b} \left(\frac{d}{2} \right) a^2 + \frac{(1-\beta)a^3}{3EI_b} \right) V_{pd} \tag{4}$$

Based on both components (u_B and v_B) of the haunch tip displacement, the shortening of the haunch flange, δ_h, is:

$$\delta_h = \sqrt{(a-u_B)^2 + (b-v_B)^2} - l_{hf} \approx u_B \cos\theta + v_B \sin\theta \tag{5}$$

where l_{hf} (= $a/\cos\theta$) is the haunch flange length.

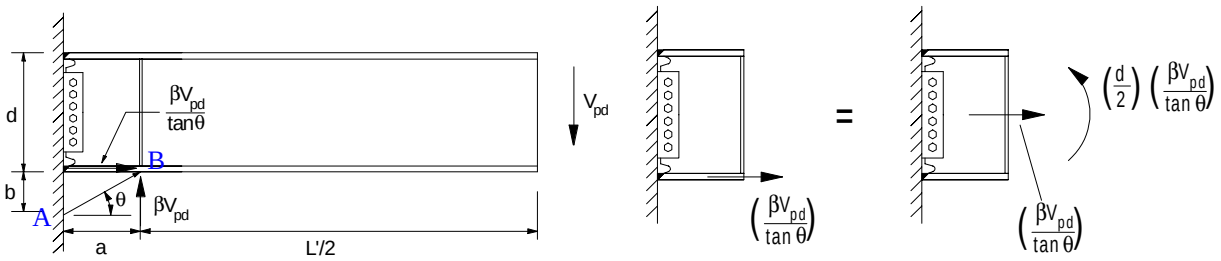

(a) Free Body Diagram of the Beam (b) Eccentric Force Due to Strut Action

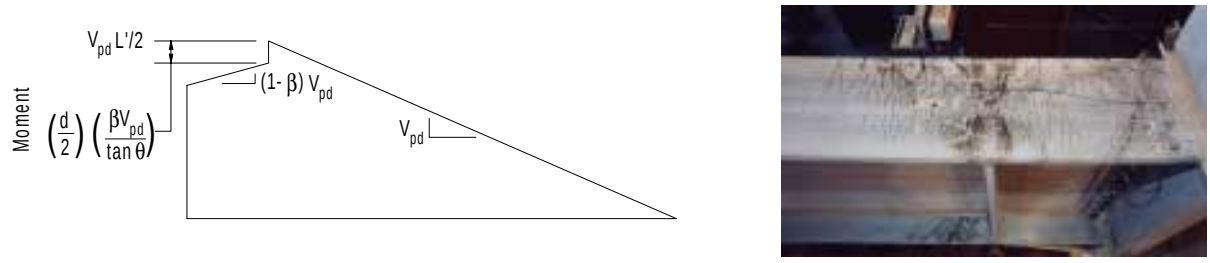

(c) Reduction of Moment due to Eccentric Force (d) Yielding Pattern of NIST-2 Beam 2

Figure 9: Free Body and Moment Diagram of Welded Haunch Reinforced Beam

The axial shortening of the haunch flange can also be established by considering the haunch flange as a free body. Since the vertical component of the haunch flange force is βV_{pd}, the axial force in the haunch flange is equal to $\beta V_{pd}/\sin\theta$, and the corresponding axial shortening is:

$$\delta_h = \frac{\beta V_{pd}}{EA_{hf}\sin\theta} l_{hf} \tag{6}$$

Equating Eqs. (5) and (6) for deformation compatibility gives:

$$\beta = \frac{b}{a} \left(\frac{3L'd + 3ad + 3bL' + 4ab}{3d^2 + 6bd + 4b^2 + \frac{12I_b}{A_b} + \frac{12I_b}{A_{hf}\cos^3\theta}} \right) \tag{7}$$

Tensile Stresses in Beam Flange Groove Welds

Since the majority of the beam shear is transferred through the haunch flange to the column, for design purposes, the beam top flange stress (i.e., the tensile stress in the groove weld) at the column face can be calculated by beam theory as follows:

$$f_{wt} = \frac{V_{pd}\, L'/2 + V_{pd}(1-\beta)a}{I_b}\left(\frac{d}{2}\right) - \frac{(\beta V_{pd}/\tan\theta)}{I_b}\left(\frac{d^2}{4} - \frac{I_b}{A_b}\right) \tag{8}$$

Defining M_{pd} as the design moment of the beam at the haunch tip, the corresponding beam shear, V_{pd}, is equal to $M_{pd}/(L'/2)$. Substituting the bending moment at the haunch tip ($V_{pd}L'/2$) by M_{pd}, the above equation can be re-written as follows:

$$f_{wt} = \frac{M_{pd} + V_{pd}(1-\beta)a}{I_b}\left(\frac{d}{2}\right) - \frac{\beta V_{pd}/\tan\theta}{I_b}\left(\frac{d^2}{4} - \frac{I_b}{A_b}\right) \tag{9}$$

The beam bottom flange force, P_{bf}, to the left of the haunch tip (point B) is much smaller than that in the top flange due to the contribution of the horizontal component of the haunch flange force [see **Figure 9**(b)]. To compute the maximum tensile stress in the beam bottom flange groove weld when the beam is subjected to positive bending, i.e., when V_{pd} in **Figure 9**(a) acts upward, the following equation can be derived with minor modifications of (8):

$$f_{wb} = \frac{V_{pd}\, L'/2 + V_{pd}(1-\beta)a}{I_b}\left(\frac{d}{2}\right) - \frac{(\beta V_{pd}/\tan\theta)}{I_b}\left(\frac{d^2}{4} + \frac{I_b}{A_b}\right) \tag{10}$$

The flexural stress profiles of the beam based on (9) and (10) are compared with those predicted by the simple beam theory and the finite element analysis in **Figure 10**. Good correlation between the proposed model and the finite element model indicates that (9) and (10) can be used reliably for design purposes.

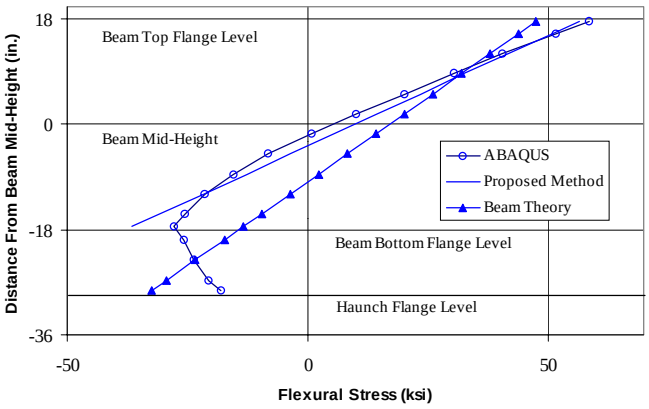

Figure 10: **Verification of Proposed Method Based on Simplified Model**

Sizing Triangular Haunch

Preliminary Haunch Geometry

In the tests conducted to date, two geometrical parameters for the majority of test specimens, a and θ [see **Figure 9**(a)], have varied only to a small extent. It seems prudent to remain within the limits of experimental database. To begin a trial design, it is suggested that the length, a, and angle, θ, of the haunch be taken as [Gross et al. 1999]:

a = (0.5 to 0.6) d (11)

$\theta = 30° \pm 5°$ (12)

The designer may want to check the value of b ($a\tan\theta$) to ensure that the haunch does not interfere with the ceiling.

Sizing Haunch Flange

For economical reasons, it is not desirable to modify the existing beam flange groove welds. The test results have shown that brittle fracture of the beam top flange groove weld did not occur when the composite slab was present even though strain gage measurements indicated that the beam top flange not only yielded but also strain-hardened. Based on strain gage measurements of the welded haunch specimens, the beam top flange strain near the column face was found to approach 20 to 30 times the yield strain. Since the actual yield strength of the beam flange was about 49 ksi, the tensile stress in the beam top flange and its groove weld (with E7XT-X electrode) might have exceeded 55 ksi under cyclic loading. Therefore, it is recommended that the allowable stress (F_w) for the existing groove welds be taken as $0.8F_{EXX}$, where F_{EXX} is the strength of the weld metal [Gross et al. 1999]. For a 70 ksi tensile strength electrode, this requirement would limit the allowable stress in the groove weld to 0.8×70 = 56 ksi.

When sizing the haunch flange to limit f_{wt} to the allowable stress, the minimum value of β can be solved by equating (9) to the allowable weld stress, F_w:

$$\beta_{\min} = \frac{(M_{pd} + V_{pd}a)/S_x - F_w}{\frac{V_{pd}a}{S_x} + \frac{V_{pd}}{I_b \tan\theta}\left(\frac{d^2}{4} - \frac{I_b}{A_b}\right)} \tag{13}$$

The haunch flange axial force, P_{hf}, is equal to $\beta V_{pd}/\sin\theta$, and once the minimum value of βV_{pd} is determined, the haunch flange can be sized as follows:

$$A_{hf} \geq \frac{P_{hf}}{\phi F_y} = \frac{\beta V_{pd}}{\phi F_y \sin\theta} \tag{14}$$

where A_{hf} = haunch flange area = $b_{hf}t_{hf}$, b_{hf} = haunch flange width, t_{hf} = haunch flange thickness, ϕ = 0.9, and F_y = minimum specified yield stress of the haunch flange. The haunch flange should satisfy the following width-thickness requirement for a compact section [*Seismic* 1997]:

$$\frac{b_{hf}}{2t_{hf}} \leq \frac{52}{\sqrt{F_y}} \tag{15}$$

In addition to satisfying the strength requirement in (14) and the stability requirement in (15), it is necessary to check the axial stiffness of the selected haunch flange to ensure that the actual β value, as computed from (7), is not less than β_{min}. If the haunch flange is conservatively designed, the actual β value will be significantly larger than β_{min}. In such case, the designer may consider reducing the haunch flange area.

Sizing Haunch Web

Note that the contribution of the haunch web is excluded in the force equilibrium in **Figure 9**(b) because its stiffness in the haunch flange direction is small. However, the haunch web plays an important role to provide stability for the haunch flange. For design purposes, it is suggested that the thickness of the haunch web satisfy the following requirement:

$$\frac{a\sin\theta}{t_{hw}} \leq \frac{260}{\sqrt{F_y}} \tag{16}$$

The above requirement is established by treating the haunch as half of a wide-flange beam section whose depth is twice the distance of $a\sin\theta$; the limiting width-thickness ratio, $2a\sin\theta/t_{hw}$, would be $520/\sqrt{F_y}$ per AISC Seismic Provisions for Structural Steel Buildings [1997].

CONCLUSIONS

A total of two pre-Northridge two-sided steel moment frame connection specimens, each comprising a W14×426 column (A572 Gr. 50 steel) and two 36×150 beams (A36 steel), was tested cyclically to study the effectiveness

of welded haunch scheme for seismic rehabilitation. One specimen incorporated an 8-ft wide lightweight concrete slab. The following conclusions can be made for the particular specimen sizes studied.

1. Welding a triangular haunch to the beam bottom flange significantly improved the cyclic performance. Although welded joints of top flanges still suffered brittle fracture for the bare steel specimen, the other specimen with a composite slab did not experience brittle fracture and was able to develop plastic rotations of 0.027 radian. Based on the satisfactory full-scale cyclic testing results, it can be concluded that welded haunch scheme is a feasible solution for seismic rehabilitation.
2. For the particular beam size (W36×150) tested, the presence of an 8-ft wide concrete slab increased the positive flexural strength by about 10% on average. No strength increase occurred in the negative bending direction, indicating that the concrete slab with welded wire mesh as reinforcement was not able to reduce the seismic force demand in the beam top flange. The presence of a concrete slab would alter the beam buckling mode. Lateral-torsional buckling was prevented due to the bracing effect of the slab, but flange local buckling still could be developed under positive bending. Therefore, strength degradation due to buckling was significantly less severe in positive bending than in negative bending.
3. The presence of a welded haunch dramatically changes the beam shear force transfer mechanism. The conventional beam theory cannot provide a reliable prediction of stress distributions in the haunch connection. Both theoretical studies and experimental results have shown that the majority of the beam shear is transferred to the column through the haunch flange rather than through either the beam web bolted connection or the beam flange groove welds. This strut action alters the moment distribution of the beam in the haunch region.
4. Providing sufficient axial stiffness and strength to the haunch flange, the force demand in the existing bottom flange groove weld is significantly reduced, and the force demand in the existing top flange groove weld can be reduced to a reasonable level. The haunch web has a minor effect on the flexural stress distribution in the beam. However, it is needed to stabilize the haunch flange.
5. A simplified model which considers both the force interaction and deformation compatibility between the beam and the haunch was developed. The predicted beam flexural stress distribution near the column face correlated well with the finite element analysis results. The model could also be used to explain the "reverse" beam shear phenomenon that was observed in testing. Based on the simplified model, a brief design procedure is proposed for sizing a triangular haunch.

ACKNOWLEDGMENTS

The research was funded by National Institute of Standards and Technology (NIST), with Dr. J. Gross as the project manager. Additional financial support was provided through AISC by the Northridge Steel Industry Fund. Steel materials and electrodes were donated by the Structural Shape Producers Council (SSPC) and the Lincoln Electric Company. The authors also like to acknowledge Professor M. D. Engelhardt, Professor K. Kasai, Mr. J. O. Malley, Mr. A. Sadre, and Mr. P. M. Hassett for providing technical advice throughout the testing program.

REFERENCES

ABAQUS User's Manual, Vols. I and II. (1995). Version 5.6, Hibbitt, Karlsson & Sorensen, Inc., Providence, RI.

Civjan, S. and Engelhardt, M.D. (1998), "Experimental Investigation of Methods to Retrofit Connections in Existing Seismic-Resistant Steel Moment Frames." *Summary Final Report* to the National Institute of Standards and Technology, Phil M. Ferguson Structural Engineering Laboratory, The University of Texas at Austin, TX.

Guidelines for Cyclic Seismic Testing of Components of Steel Structures for Buildings. (1992), Report No. ATC-24, Applied Technology Council, Redwood City, CA.

Gross, J.L., Engelhardt, M.D., Uang, C.-M., Kasai, K., and Iwankiw, N. (1999), "Modification of Existing Welded Moment Frame Connections for Seismic Resistance." To be published by AISC.

Interim Guidelines: Evaluation, Repair, Modification and Design of Welded Steel Moment Frame Structures. (1995), FEMA267, SAC Joint Venture, Sacramento, CA.

Seismic Provisions for Structural Steel Buildings. (1997), 2nd Ed., AISC, Chicago, IL.

Uniform Building Code (UBC). (1985). Int. Conf. Bldg. Officials, Whittier, CA.

Yu, Q.-S., Noel, S., and Uang, C.-M. (1997), "Experimental and Analytical Studies on Seismic Rehabilitation of Pre-Northridge Steel Moment Connections: RBS and Haunch Approaches." *Report No. SSRP-97/08*, Division of Structural Engineering, University of California, San Diego, La Jolla, CA.